Vibration Analysis and Rock Debris in the Rock Drilling Process

Mária Bali Hudáková[1*)], Víťazoslav Krúpa[2)], Alexander Kiovský[3)], Pavol Vavrek[4)], Edita Lazarová[5)], Lucia Ivaničová[6)]

[1*)] Institute of Geotechnics of the Slovak Academy of Sciences, Watsonova 45, SK-04001 Košice, Slovakia; E-mail: krulakova@saske.sk; https://orcid.org/0000-0002-3897-4762
[2)] Institute of Geotechnics of the Slovak Academy of Sciences, Watsonova 45, SK-04001 Košice, Slovakia; E-mail; krupa@saske.sk; https://orcid.org/0009-0004-5030-0914
[3)] Institute of Geotechnics of the Slovak Academy of Sciences, Watsonova 45, SK-04001 Košice, Slovakia; E-mail; kiovsky@saske.sk; https://orcid.org/0009-0002-7278-0360
[4)] Institute of Geotechnics of the Slovak Academy of Sciences, Watsonova 45, SK-04001 Košice, Slovakia; E-mail; vavrek@saske.sk; https://orcid.org/0000-0002-1125-1361
[5)] Institute of Geotechnics of the Slovak Academy of Sciences, Watsonova 45, SK-04001 Košice, Slovakia; E-mail; lazarova@saske.sk; https://orcid.org/0000-0003-4682-6433
[6)] Institute of Geotechnics of the Slovak Academy of Sciences, Watsonova 45, SK-04001 Košice, Slovakia; E-mail; ivanic@saske.sk; https://orcid.org/0000-0003-3844-9703

https://doi.org/10.29227/IM-2026-02-02-052

Submission date: *2026-09-04* | Review date: *2026-24-04*

Abstract

This study analyzes laboratory rock drilling of andesite and limestone using an experimental drilling rig. The description of mechanical rock disintegration was based on defining the properties of the drilled rocks, describing the measured vibrations, calculating the output parameters of the rock disintegration, and comparing them under different drilling regimes using the same drilling tool. Experiments were conducted using two three-channel surface-set diamond core drill bits with identical diamond sizes. The rock disintegration performance was assessed using the measured output variables, which were torque and penetration rate of the drill bit. From these, the specific energy and drilling strength were calculated. Vibration diagnostics were based on the measured vibration acceleration signal. The primary aim of the experimental research was to gain insight into how changes in thrust force and rotational speed (controllable input variables) affect the size of the drill debris and vibrations for the selected rock-tool system. The energy intensity of drilling andesite and limestone was evaluated using specific energy and rock debris. The rock debris was assessed using the coarseness index CI and the absolute size constant d', employing the Rosin–Rammler method. Comparing drilling into two different types of rocks, limestone and andesite, resulted in a more precise classification of the rock debris, vibration emissions, and their relationships. The drilling of andesite and limestone was analyzed by calculating the overall vibration level in the 4,000-9,000 Hz frequency range using the power spectral density function. This evaluation considered variations in the constant drilling regime and was compared with the specific energy values obtained and the calculated inflection point. The inflection point indicates the start of the efficient disintegration region, where chipping occurs. It was found that evaluating only axial vibrations to describe the rock disintegration region is insufficient; it is also necessary to monitor lateral and torsional vibrations for a more comprehensive understanding of the rock-tool interaction. The results included comparisons of the power spectral density in the high-frequency range with the coarseness index (CI) and the ratio of specific energy to drilling strength. In the high-frequency range of 6,500 Hz, the rock-tool interaction was characterized by higher power spectral density, increased coarseness index, and decreased drilling strength observed during limestone drilling.

Keywords: *rock drilling, rock debris, power spectral distribution, coarseness index*

1. Introduction

During drilling, disintegration occurs when rock separates from the massif or breaks apart when its strength is exceeded. At low pressures under the contact surface of the drilling tool, the rock is crushed, with the diamond core working in a so-called surface-abrading mode. At very high pressures, when the flushing fluid cannot remove the disintegration products, the diamond drill bit switches to a secondary crushing mode of the already disintegrated rock. The highest probability of volumetric disintegration is defined by the interval of external force load $F \in \langle F_{inf}, F_2 \rangle$, where the inflection point F_{inf} was calculated from the S-curve of the penetration depth [1]. To analyze the entire rock disintegration process, it is essential to identify which of the described failure zones the measured vibration signal falls within. Conditions for measuring the vibration signal must be maintained in accordance with the selected measurement chain configuration to ensure high-quality, comprehensive vibration diagnostics.

Based on rock type and changes in drilling regime parameters, it is possible to determine optimal system settings that minimize energy consumption and identify the area of volumetric disintegration. This issue is very complex because it requires consideration of numerous factors within the system, including torque T (Nm), drilling advance rate, rotational speed n, pressing force F, properties of the fractured rock environment, and properties of the drilling tool. The research is based on the assumption that the vibrational effect during drilling is specific to each rock type [2], [3]. Sources of vibrational emission during rock drilling can be much more difficult to identify, especially given the heterogeneity of the disintegrated material, the more complex crystalline structure, and the changing disintegration mechanisms under different drilling regimes.

Figure 1 shows a simple schematic of a dynamic system comprising an indenter and a rock, which are affected by two main input variables: thrust force and rotational speed (drill bit revolutions). The measured outputs of this system include operational quantities such as torque, power, and drilling rate, which can be observed over time, along with the vibration signal. The system also receives 'faults,' either controllable (e.g., indenter type, rock type) or uncontrollable (e.g., indenter properties, rock properties, and so on).

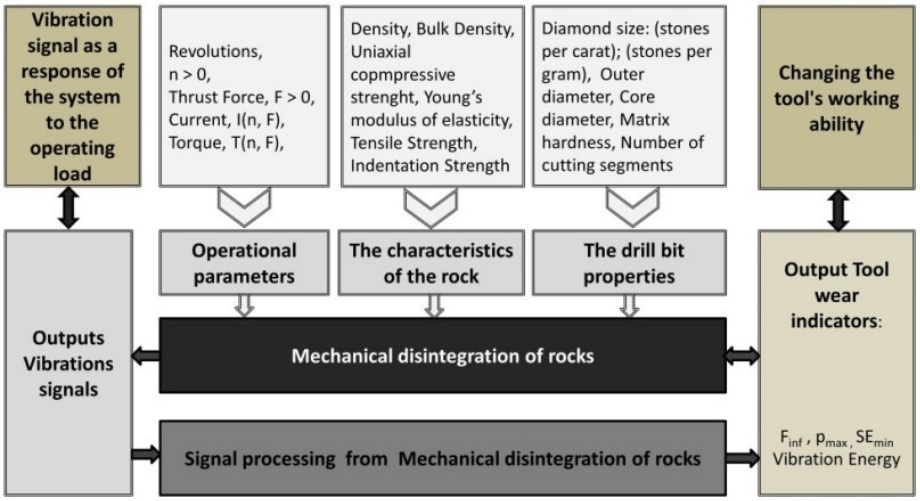

Fig. 1. Scheme for preprocessing and analyzing regime parameters and vibration signals during rotation drilling of rocks.

The power demand during vibration diagnostics assumes that active power, similar to instantaneous power, derives from analog signals. This power reflects the average of the instantaneous power, with 'active' indicating the portion that does work, showing how much of the original electrical energy is transformed into another form—in this case, vibrational energy.

Both the average and root-mean-square amplitudes express the total energy of the process. Variability in the amplitude over time, or in its distribution, represents the dynamics of friction. The amplitude distribution of pulses reveals the energy of the vibro-acoustic emission (VAE) source, while the amplitude distribution provides information about the source's energy distribution [4], [5].

Just as the rock disintegration mechanism varies, the properties of the fractured rock under different drilling regimes also influence the formation of drilling debris. Rock debris reflects the drill's efficiency and performance. Rock debris and its monitoring can help in choosing the appropriate drilling tool. Evaluation of rock debris can help select the appropriate drilling machine and drill bit. The production of more fine debris indicates improper drill and bit selection [6], [7].

This article analyzed the processes of rock disintegration and mechanical vibration from recorded vibration acceleration signals during drilling into limestone and andesite. Changing the drilling regime parameters allowed us to monitor their impact on the vibration signal and the output variables from the drilling process. The monitored output variables included analysis of drill cuttings, vibration signals, and output parameters calculated after drilling the rock sample.

2. Laboratory experimental part and methods

The experimental horizontal drilling rig was designed as a dynamic system with two controllable input parameters – thrust force F (N) and drill bit revolutions n (rpm). The system outputs include the torque of the 3-phase motor T (Nm), the torque of the drill bit $T_{kistler}$ (Nm), the drilled length L (m), and the acceleration of the vibration signal (m/s^2). Torque of drill bit $T_{kistler}$ (Nm) and cutting forces (F_x, F_y, F_z) in rock drilling measured by 4-component dynamometer Kistler 9272, providing three orthogonal force components and torque, along with a multichannel charge amplifier for multicomponent force measurement Kistler 5070. Vibrations generated during drilling were measured using piezoelectric accelerometers in the x, y, and z-directions, as shown in Fig. 2 (right).

Vibration sensors measuring the oscillatory motion of the drilling rig are mounted on the rock specimen's fixing frame. They provide data on vibration acceleration in three orthogonal directions using accelerometers Wilcoxon 784A-3 and CTC AC102-1A, integrated with the online vibration monitoring system Adash 3900-II. The X-direction aligns with the drilling direction, while the Z-direction is perpendicular to X and lies in a horizontal plane. It measures vibration acceleration in three mutually perpendicular directions: X, Y, and Z.

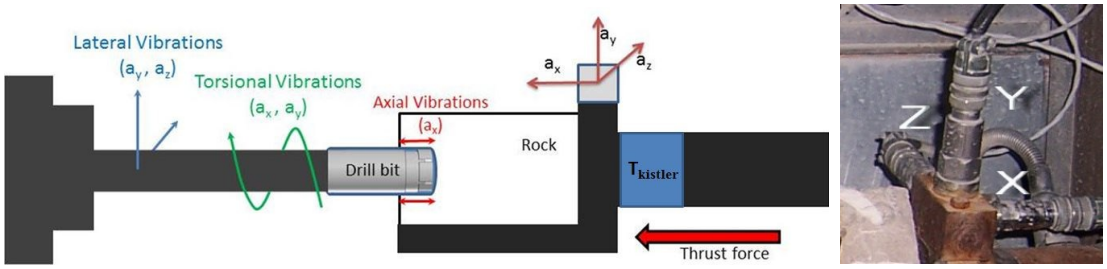

Fig. 2. Schematic illustration of the drill bit's oscillation (left) and the placement of vibration sensors (right).

Vibrations were recorded at the same sampling frequency of 18,000 Hz during drilling into both andesite and limestone. Data collection of the drilling process was carried out at 100 Hz. Synchronization of the vibration signal data sampling and mode

parameters was performed in MATLAB. Data synchronization to determine the magnitude of change was evaluated over a 1-second interval. With constant drill bit revolutions of n=200 rpm and n=700 rpm, the axial force F was gradually increased to values of 4,000N, 8,000N, and 12,000N.

Experiments were conducted using two three-channel surface-set diamond coring drill bits, each with an outer diameter of 46 mm, an inner diameter of 32 mm, and a matrix hardness of 400 HV. The diamond sizes on the drill bits were the same: 16/25 stones per carat. This type of drill bit is commonly used for core drilling in soft to medium-hard rocks.

Experiments were conducted using andesite specimens from a quarry in Ruskov, located on the volcanic mountains known as Slanske vrchy in Slovakia, and limestone specimens from a quarry in Včelare, Slovakia. Selected properties of the tested rocks are shown in Table 1. These properties were determined in accordance with the applicable standards CEN ISO/TS 17892, EN 1997–2:2007(E), and ON 441121.

Tab. 1. Properties of drilling rock specimens.

Rock specimens	Bulk density (kg. m^{-3})	UCS (MPa)	Brazilian test (MPa)	HB (kg.mm^{-2})	Punch shear (MPa)	k_p	σ_{red} (MPa)
Andesite	2,514	200.1	15.6	5921,0	24.8	1.09	11,826
Limestone	2,691	85.1	9.3	466.4	9.5	1.36	1,728

Note: *UCS - Uniaxial Compressive Strength, HB - Brinell Hardness Test, Brazilian Test - Indirect Tensile Strength, k_p - Plasticity coefficient, σ_{red} - Reduced indentation strength.*

Andesite is a compact rock, grey or brown-grey in color, and slightly or medium porphyric. Limestone is a sedimentary rock composed of calcite (calcium carbonate, CaCO3) containing iron oxide minerals. It has a relatively fine to medium-coarse texture. According to Slovak technical norm ON 441121, limestone has a defined abrasiveness value of 0.0186 mg.m^{-1} and is classified as a rock with low abrasiveness. Andesite has a defined abrasiveness value of 0.7913 mg.m^{-1} and is classified as a rock with higher abrasiveness.

According to the standard STN 72 1001 "Classification of soils and rocks", we classify limestones into class R2 - high-strength rocks, and andesites into class R1 - very high-strength rocks.

2.1 Drilling program analyzing rock debris and output parameters

Table 2 describes the applied drilling regime (rotation speed of the drill bit n and thrust force F) along with the calculated characteristics of the drilling cuttings: absolute particle size d' (μm) and Coarseness index CI for the length of the drill hole L (mm).

Tab. 2. Drilling program of drill bits 16/25.

Rock specimen	L (mm)	F (N)	n (rpm)	d' (μm)	CI
Andesite	60	0-4,000	200	40.89	191.23
Andesite	60	0-8,000	200	15.03	167.86
Andesite	100	0-12,000	200	38.30	182.76
Andesite	60	0-4,000	700	9.39	145.89
Andesite	140	0-8,000	700	27.52	170.86
Andesite	140	0-12,000	700	29.74	173.44
Limestone	60	0-4,000	200	82.90	245.54
Limestone	60	0-8,000	200	55.23	220
Limestone	100	0-12,000	200	71.85	235.96
Limestone	60	0-4,000	700	50.69	209
Limestone	140	0-8,000	700	72.06	229.78
Limestone	140	0-12,000	700	104.96	269.04

The rock debris particles were analyzed by applying a wet sieve analysis since the drilling was carried out while using water as the flushing fluid at a volumetric flushing rate of 10^{-3}m^3.s^{-1}. We determined the rock disintegration products by their characteristics, which define the particle size of the crushed material, using the calculation of the coarseness index (CI) and the absolute particle size d′.

The coarseness index (CI) values were determined for different applied regime parameters, as shown in Table 2. CI is the sum of cumulative percent by weight of the rock debris captured on each sieve used [6], [8]. CI is a non-dimensional number. The sieve analysis was carried out using sieves of the following mesh sizes: +1,000 μm; 400 μm; 200 μm; 160 μm; 80 μm; 40 μm; and -40 μm.

The absolute particle sizes d' were obtained from the Rosin–Rammler distribution function, which is one of the most widely used particle size distribution curves. The Rosin–Rammler relationship is given by equations (1) and (2):

$$R_R = 100.\exp\left[-\left(\frac{d}{d'}\right)^n\right] \tag{1}$$

$$\ln\left[\ln\left(\frac{100}{R_R}\right)\right] = n.\ln(d) - n.\ln(d') \tag{2}$$

where R_R denotes the cumulative mass (volume) as a percentage retained on the sieve of size d; d′ denotes the absolute particle size defined as the size at R_R = 36.79%; and n denotes the distribution parameter [9].

The calculation of the mutual mathematical relationships (3-5) for determining the process evaluation parameters was derived from a record in which the drilling tool's rotational speed and the applied thrust force reached their maximum values, i.e., a constant drilling regime.

The E-S diagram visually illustrates the dependence of specific energy E on drilling strength S, where both E and S have stress dimensions. The specific energy E is proportional to the torque of the drill bit, $T_{kistler}$, and the external force load F. The drilling strength S is inversely proportional to the cutting depth p [10], [11].

The specific energy E is determined by expression (3),

$$E = \frac{2\pi}{A}.\frac{T_{kistler}}{p} = \frac{2T_{kistler}}{(R^2-r^2)p} \quad (MPa) \tag{3}$$

where A (mm²) is the surface area of the cutting face of the bit, A = π. (R² – r²), R (mm) is the outer radius of the drill bit, r (mm) is the inner radius of the drill bit, p (mm) is the penetration depth (tool advancement per one rotation), and $T_{kistler}$ (Nmm) is the torque of the drill.

The drilling strength S is given by relation (4),

$$S = \frac{F}{(R-r).p} = \frac{F}{h.p} \quad (MPa) \tag{4}$$

where h (mm) is the width of the segment defined as the difference between the outer and inner radius of the drill bit.

The specific energy of drilling (SE) can also be expressed as the amount of energy consumed per unit volume (or mass unit) of disintegrated rock, where v (m/s) is the disintegration velocity, which in equation (5) is a function of the thrust force and the rotational speed of the drilling tool.

$$SE = \frac{P}{Av} = \frac{2\pi nT}{Av} \ (MJm^{-3}) \tag{5}$$

Based on energy theories of rock disintegration, we can conclude that during optimal rock drilling, most of the energy is used to create new surfaces on the resulting disintegration products and to generate heat [12]. More energy is required to produce a fine-grained disintegration product [7], [9]. This axiom is explained by several energy and technological theories of material disintegration.

2.2 Analysis of acceleration vibrations using power spectral density and acceleration vector

The power spectral density (PSD) was calculated using a bandpass filter applied to the measured acceleration signal, A_x, along the drilling axis. PSD defines how the signal's power is distributed across different frequencies, providing insight into random or periodic signals in the frequency domain. The sampling frequency of the vibration signal, f_s, was 18,000 Hz, with a Nyquist frequency of f_N = 9,000 Hz. To prevent aliasing, the sampling frequency should be at least twice the highest frequency components in the measured signal (Nyquist-Shannon sampling theorem), $f_s > 2f_{max}$; this condition was satisfied.

The total number of created frequency intervals, j, was determined by defining the frequency domain f and the bandwidth w, from which we can calculate the total signal level using equation (7). For example, if we wanted to assess the power spectrum of the acceleration of the vibration signal A_x in the frequency domain f, from 0 Hz to 9000 Hz with a set bandwidth w = 100 Hz, then the calculation of the number of intervals j would be as follows: j = (the last value of the frequency interval in Hz (9,000) - the first value of the frequency interval in Hz (0)) / w = 90.

By setting the bandwidth w to the same value, we ensure the creation of an equal increment for filtering the signal expressed in the frequency domain f ∈ <0, 1.w, 2.w, ..., j.w>, where j indicates the total number of created frequency intervals. Then, the calculation of the first mean frequency, which corresponds to the first calculated PSD value, according to equation (8), is as follows if w = 100 Hz: (0 + 1.w) / 2 = 50 Hz.

The power spectrum expresses the average power of individual frequency components (intervals). To calculate the average power (Root Mean Square (RMS)), equation (6) was used, where j describes the ordinal number of the created interval, and N indicates the number of data points corresponding to the time segment of the evaluated acceleration of the vibration signal A_x. The average power referred to here is the average amount of energy transferred or distributed over a given time interval.

$$RMS_j = \sqrt{\frac{1}{N}\sum_{i=1}^{N}(A_x)^2} \quad (m.s^{-2}) \tag{6}$$

The overall level of the vibration signal represents the total dynamic energy across a wide frequency range. Then, the total vibration signal level (m/s² RMS) was calculated using equation (7).

$$\text{Overall level} = \sqrt{\sum_{i=1}^{j}\left(RMS_j\right)^2} \quad (m.s^{-2}RMS) \tag{7}$$

The power spectral density (PSD) was calculated according to equation (8), where w is the bandwidth in Hz.

$$PSD = \frac{\left(RMS_j\right)^2}{w} \quad ((m.s^{-2})^2/Hz) \tag{8}$$

Table 3 presents the calculated overall level of the vibration signal A_x (m. s⁻² RMS) in the frequency domain, f, from 4,000 Hz to 9,000 Hz, with a bandwidth w = 100 Hz and 50 frequency intervals j. These values were derived from the recorded time interval during the constant drilling mode, including the calculated total acceleration vector magnitude ā.

The total magnitude of the acceleration vector ā is calculated from the three components of vibrational acceleration (a_x, a_y, a_z). This value was determined only from the constant mode of limestone and andesite drilling, according to equation (9),

$$\bar{a} = \frac{1}{T}\sqrt{\left(a_x^2 + a_y^2 + a_z^2\right)} \quad (m/s^2) \tag{9}$$

where T represents the duration of the constant drilling mode. The magnitude of the acceleration vector ā was calculated to capture the increase in vibrational acceleration along the Y and Z axes (Fig. 2).

Tab.3. Calculated characteristics for measured mechanical accelerations of vibration signals.

Applied regime (F/n)	Limestone Overall level A_x (m/s^2RMS)	Limestone ā (m/s^2)	Andesite Overall level A_x (m/s^2RMS)	Andesite ā (m/s^2)
4kN/700 rpm	21.16769	43.7765	25.88035	44.27453
8kN/700 rpm	57.42087	59.30699	39.64228	58.20239
12kN/700 rpm	39.69217	58.23393	39.10137	55.90592
4kN/200 rpm	16.50075	16.83461	7.367713	13.02047
8kN/200 rpm	6.342162	12.86855	11.32641	17.75998
12kN/200 rpm	22.45492	20.56392	10.24706	13.73897

Tables 4 and 5 present the calculated PSD values ((m/s²) ²/Hz) of the filtered vibration signal A_x for limestone and andesite in the drilling direction, for the frequency domain f from 0 Hz to 9000 Hz, with a bandwidth setting w=1000 Hz. A total of nine frequency intervals were created. Tables 4 and 5 display three intervals: two are low-frequency (1500 Hz and 2500 Hz), and one is high-frequency (6,500 Hz). These PSD values were derived from the rotational movement induced by gradually increasing the thrust force up to its set constant level, during constant rotation of the drill bit. The vibration acceleration analysis was performed from the overall time record of drilling the rock sample.

Tab. 4. Power spectral density PSD ((m/s²) ²/Hz) of filtered vibration signal A_x for limestone.

Applied regime (F/n)	frequency 1,500 Hz	frequency 2,500 Hz	frequency 6,500 Hz
4kN/700 rpm	1.096	0.141	0.241
8kN/700 rpm	0.994	0.262	1.26
12kN/700 rpm	1.33	0.267	0.661
4kN/200 rpm	0.052	0.0149	0.1499
8kN/200 rpm	0.0928	0.032	0.02169
12kN/200 rpm	0.08	0.0329	0.207

Tab. 5. Power spectral density PSD ((m/s²) ²/Hz) of filtered vibration signal A_x for andesite.

Applied regime (F/n)	frequency 1,500 Hz	frequency 2,500 Hz	frequency 6,500 Hz
4kN/700 rpm	1.25	0.08	0.34
8kN/700 rpm	1.83	0.14	0.787
12kN/700 rpm	1.84	0.189	1.27
4kN/200 rpm	0.064	0.0028	0.027
8kN/200 rpm	0.172	0.0401	0.077
12kN/200 rpm	0.047	0.0074	0.0512

Based on the data from Table 5, we can conclude that PSD increases during drilling of andesite with higher drill bit speeds (n) and increasing thrust force (F) across all frequency ranges. During limestone drilling, the PSD distributed between lower and higher frequencies does not follow this trend, as shown in Table 4.

3. Analysis of regime parameters used for drilling in andesite and limestone

In terms of evaluating the applied thrust force F(N) and the drill bit revolutions n (rpm) when drilling into limestone and andesite, it can be stated that with increasing thrust force, the drilling speed v (mm/s) increased for both drilled rocks, see Fig. 3. The drilling speed reached higher values when drilling into limestone, Fig. 3.

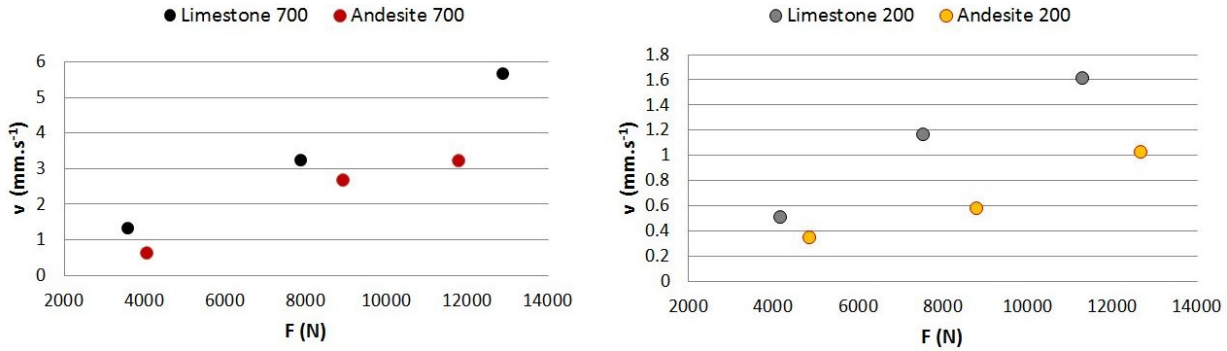

Fig. 3. Average drilling speed dependent on thrust force F and drill bit revolutions n=700 rpm (left) and n=200 rpm (right).

From the graph of the specific energy dependence on the applied thrust force, we found that during limestone drilling, the values of specific energy were half as low as those for andesite, even after increasing the drill bit revolutions, Fig. 4. Therefore, the amount of energy consumed for rock disintegration is not only a property of the material being broken but also a function of the process.

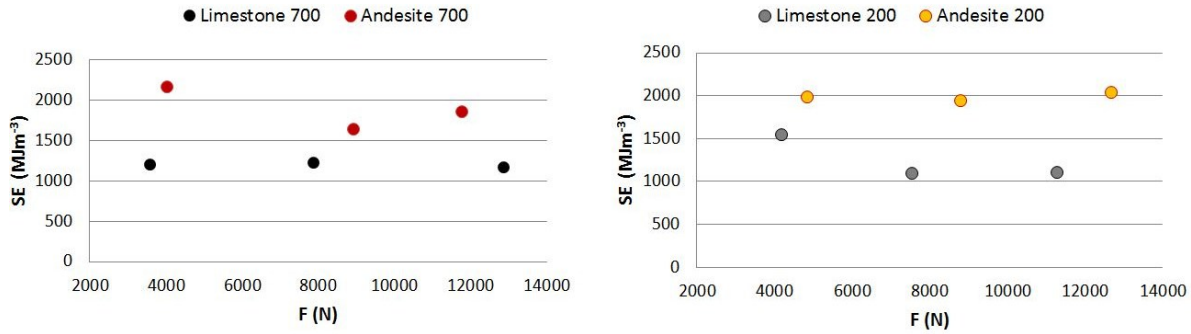

Fig. 4. Average specific energy dependent on thrust force F and drill bit revolutions n=700 rpm (left) and n=200 rpm (right).

Before assessing the maximum efficiency of the rock disintegration process, we also considered a parameter representing the ratio of drilling speed to specific energy, v/SE. This parameter indicates the achieved drilling speed per unit of specific energy. We also refer to this parameter as the tool's working ability, φ. Figure 5 shows that the used drilling bit is better suited to limestone. When drilling andesite, the φ value reaches half its maximum at increasing applied thrust force and at higher rotational speeds of the drill bits.

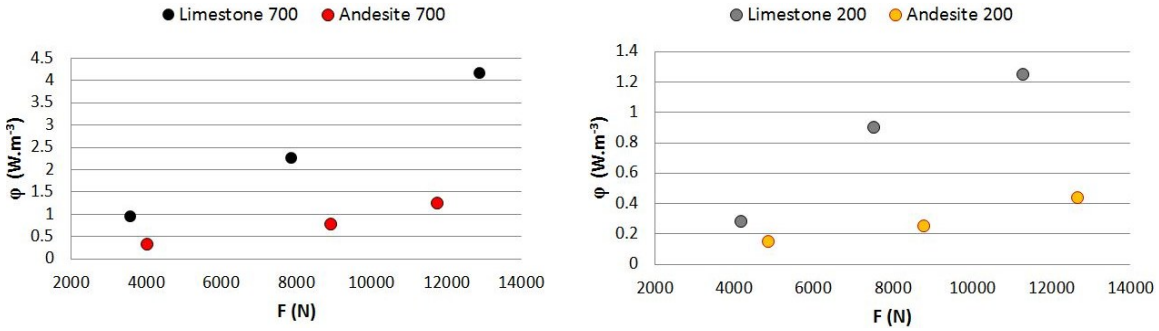

Fig. 5. Average tool's working ability depending on increasing applied thrust force F and drill bit revolutions n=700 rpm (left) and n=200 rpm (right)

3.1 The final analysis of rock debris and vibration signals for evaluating the rock disintegration process

From the perspective of external force loading, we can describe the rock disintegration mechanism using the inflection point F_{inf}, which marks the beginning of the volumetric rock disintegration region. Figure 6 shows the shift in the start of the volumetric disintegration region to higher thrust force F with increasing axial vibration amplitude A_x and drill bit revolutions from 200 rpm to 700 rpm (see Tab. 3).

Figure 6 also shows the onset of volumetric rock disintegration at an applied thrust force of F=4 kN for both drilled samples, but the maximum level of total vibration A_x was reached in andesite and limestone at an applied pressure of 8 kN.

At lower drill bit revolutions (200 rpm) with an increasing inflection point, the overall level of axial vibrations Ax, measured in the frequency spectrum from 4 kHz to 9 kHz, increased for andesite to 11.326 (m/s² RMS), while for limestone it decreased to 6.34 (m/s² RMS), as shown in Fig. 6. When using higher drill bit revolutions (700 rpm) and increasing the thrust force, an increase in the inflection point was also recorded for both drilled rocks. A more significant decrease in the overall vibration level of axial vibrations A_x was observed at a thrust force of 12 kN for limestone, which could have been caused by an increase in the coarseness coefficient CI, see Tab. 2, and an increase in torsional and lateral vibrations, considering the calculated magnitude of the acceleration vector ā, listed in Table 3.

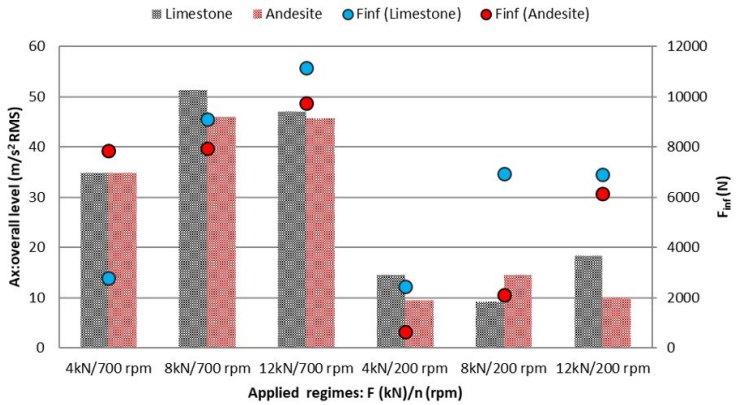

Fig. 6. Applied drilling regimes and calculated overall vibration levels A_x from the constant drilling mode and the inflection points F_{inf}, see Tab.3

Figure 7 shows a decrease in the average specific energy SE, while the overall vibration level A_x (m/s² RMS) increases during drilling of andesite at two thrust force levels (4 kN and 8 kN) with a constant drill bit rotation speed (700 rpm). At higher drill bit revolutions (700 rpm) and higher applied thrust force, specific energy remained nearly constant during limestone drilling. At the same time, the overall vibration A_x (m/s² RMS) increased at both thrust force levels of 4 kN and 8 kN, as shown in Fig. 7. At lower

drill bit revolutions (200 rpm), the highest value of overall vibration A_x (m/s² RMS) was observed at an applied thrust force of 12 kN for limestone and at 8 kN for andesite. The minimum value of specific energy was recorded for limestone and andesite at a thrust force of 8 kN.

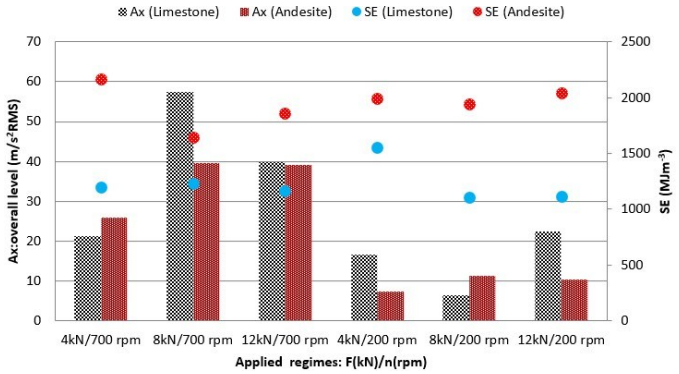

Fig. 7. Applied constant drilling regimes and overall vibration emission power levels in the drilling direction A_x, and average specific energy SE, see Tab. 3.

This identification of the rock disintegration mechanism in the initial phase of volumetric disintegration, based on comparing the overall level of axial vibration performance (A_x) with the specific energy (Fig. 6 and Fig. 7), is not entirely reliable for accurately determining how the rock interacts with the tool.

It concerns the transmitted power from the drilling tool, driven by an electric motor via a belt drive. This power needs to be monitored using a three-dimensional representation of the vibration signal. Nevertheless, as a suitable method for defining the disintegration regime, the calculated spectral power density (PSD) in the high-frequency range (6,500 Hz), where the interaction between the rock and the tool was determined, along with the calculated E-S values (equations 3-4), appears promising. The calculated coarseness index CI values indirectly reflect the efficiency and performance of the drilling tool, as shown in Figures 8 and 10.

Figure 8 shows the dependence of the E/S ratio and the coarseness index CI during drilling into andesite and limestone; see Table 2. The calculated E and S values were obtained from a constant drilling regime. E/S ratio and coarseness index CI are non-dimensional numbers.

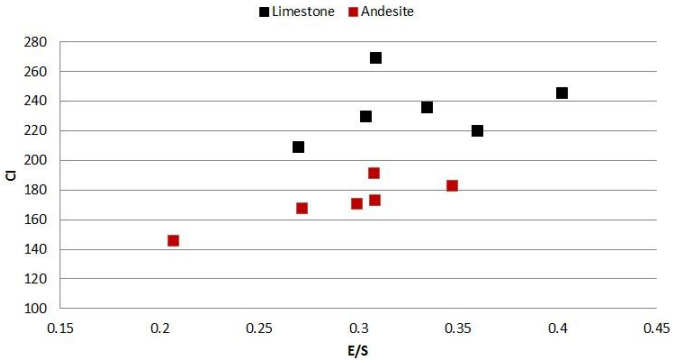

Fig. 8. The relationship between the E/S ratio and the CI coarseness index

Reducing the coarseness index means that after drilling the andesite, the specific energy E increased with increasing thrust force. This indicates that rock disintegration with a higher coarseness index requires lower specific energy E and lower force load S per unit of disintegrated limestone rock sample compared to andesite. In the plot in Fig. 9, a decrease in power spectral density and an increase in the E-S ratio were observed during drilling of both rock samples, as shown in Tables 4 and 5.

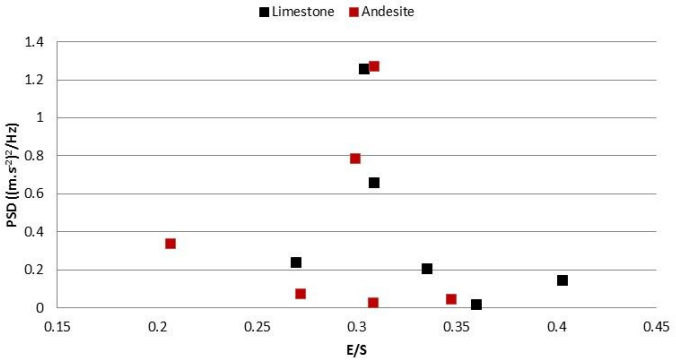

Fig. 9. Relationship between the E/S ratio and the power spectral density (PSD) in the high-frequency range (6,500 Hz).

Two different rock types produced varying particle sizes of rock debris during drilling, which influenced the axial and torsional vibrations of the drill rig.

The lower coarseness index values compared to limestone, as shown in Table 2, resulted in a lower increase in axial vibrations, as shown in Tables 4 and 5.

In Figure 10, the value of the coarseness index was compared with the achieved value of the power spectral density in the frequency interval f = 6,500 Hz. From the dependence shown in Figure 10 (left), it is evident that as the power spectral density increases, the coarseness index CI also increases at higher drill bit rotation speeds during drilling into andesite.

For limestone, the power spectral density decreased at an applied thrust force of 12 kN, which could have caused an increase in torsional and lateral vibrations, considering the calculated overall magnitude of the acceleration vector ā, shown in Table 3, and a significant increase in the coarseness index and the absolute particle size d', listed in Table 2.

At lower drill bit revolutions in Figure 10 (right), the power spectral density decreased with increasing coarseness index in the andesite. For limestone, the decrease in PSD was only recorded with an increase in the coarseness index at an applied thrust force of 8 kN, which could have led to an increase in torsional and lateral vibrations, considering the calculated overall magnitude of the acceleration vector ā and the overall level of axial vibrations A_x, as shown in Table 3.

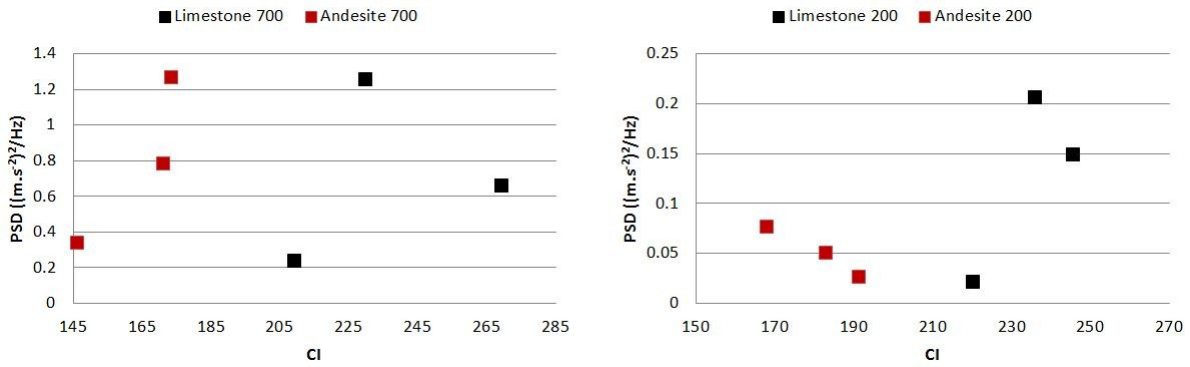

Fig. 10. The relationship between the power spectral density (PSD) in the high-frequency range (6,500 Hz) and the coarseness index CI with changing drill bit revolutions n: 700 rpm (left) and 200 rpm (right) from the complete vibration record.

When rock debris particles are too large, they significantly reduce the drill bit's axial vibration but increase wear and stick-slip vibrations. Conversely, very small particles can reduce wear and sticky vibrations without halting the drill bit's axial rough drilling, though this often results in decreased chip removal efficiency. Therefore, during field studies of rock-cutting transport, it is crucial to carefully consider factors related to drilling string vibration and to choose a suitable particle size and rock-carrying efficiency [13].

4. Conclusion

During the evaluation of the energy model, experimentally measured data relationships to work points were used, which were determined by the applied thrust force and drill bit revolutions. From the perspective of assessing the applied thrust force and the rotational speed of the drilling tool during drilling into limestone and andesite, it can be stated that with increasing thrust force, the drilling speed and the tool's working ability increased linearly in both types of rock. Based on comparisons of vibration measurements obtained with accelerometers, we can conclude that, in terms of the energy response of oscillations along the drilling axis and the achieved minimum specific energy, the rock-drilling process is random and influenced by the rock environment and the drilling regime. When drilling limestone and andesite samples, increasing torsional and lateral vibrations reduced the coarseness index at lower drilling tool rotational speeds and an applied thrust force of 8 kN.

During drilling into limestone and andesite samples at higher drill bit revolutions and an applied thrust force of 12 kN, the torsional and lateral vibrations increased, along with the coarseness index CI and the absolute particle size d'. Drilling two rock samples produced fragments of different sizes, which could have influenced axial and torsional vibrations during drilling.

A decrease in the spectral power density at high-frequency ranges and an increase in the E-S ratio were observed during the drilling of both rock samples. These findings can help determine the rock environment during drilling by measuring output variables such as specific energy and drilling strength, as well as high-frequency vibration emissions. Each rock environment has its own specific characteristics, including rock debris, which depend on the drilling tools used and the recorded vibrations.

Acknowledgments

This research was supported by projects VEGA 2/0090/23 and APVV-23-0364.

References

1. V. Krúpa, M. Kruľáková, E. Lazarová, M. Labaš, K. Feriančiková, L. Ivaničová, "Measurement, Modelling and Prediction of Penetration Depth in Rotary Drilling of Rocks", Measurement 117, 165-175 (2018)
2. Z. Li and K. Itakura, "Modeling and simulation of the effect of rock grain sizes on vibration characteristics when rock drilling," in 11th Conference of Asian Rock Mechanics Society 21-25 October 2021, IOP Conference Series: Earth and Environmental Science 861.
3. E. Lazarová, M. Kruľáková, V. Krúpa, M. Labaš, K. Feriančiková, "Regime and rock identification in disintegration by drilling based on vibration signal differentiation," International Journal of Rock Mechanics and Mining Sciences 149, 104984 (2022).
4. V. Baranov, E. Kudryavtsev, G. Sarychev, V. Schavelin, "Acoustic Emission in Friction", Vol. 53 of Tribology and Interface Engineering, Elsevier Science, 2007.

References

5. A. Le Bot and E. Bou Chakra, “Measurement of Friction Noise Versus Contact Area of Rough Surfaces Weakly Loaded”, Tribology Letters 37 (2), 273-281 (2010).
6. S. Kumar, R. Talreja, V.M.S.R. Murthy, “Development of a drill energy utilization index for aiding selection of drill machines in surface mines”, Int. J. Min. Sci. Technol. 27, 393–399 (2017).
7. M.B. Hudáková, A. Kiovský, V. Krúpa, P. Vavrek, E. Lazarová, L. Ivaničová, “The Evaluation of the Wear of Surface-set Diamond Drill Bits by Analysing the Rock Debris and Process Parameters”, Inz. Miner. 3(2), (2025).
8. F.F. Roxborough and A. Rispin, “The mechanical cutting characteristics of the Lower Chalk”, Tunnels and Tunnelling, 45-67 (1973).
9. H.-E. Kim, K.-M. Nam, H. Rehman, T.-S. Kyeon, H.-K. Yoo, “Comparison Study on Coarseness Index and Maximum Diameter of Rock Fragments by Linear Cutting Tests”, Applied Sciences 12(17), 8793 (2022).
10. E. Detournay, T. Richard, M. Shepherd, “Drilling response of drag bits: Theory and experiment”, International Journal of Rock Mechanics and Mining Sciences 45(8), 1347–1360 (2008).
11. V. Krupa, M. Bali Hudáková, E. Lazarova, P. Vavrek, A. Kiovsky, L. Ivaničova, “Interpretacija rezultata bušenja krečnjaka korišćenjem E - S dijagrama”, Rudarski glasnik 122(1-2), 63-76 (2025).
12. F. Sekula, V. Krúpa, O. Krajecová, M. Merva, “Energeticko-transformačné merania v procese vŕtania pri určovaní mechanickej anizotropie hornín”, Rudy 27, 86-90 (1979).
13. X. Guo, S. Xiao, X. Qiu, X. et al., “Experimental investigation on axial–torsional coupling nonlinear vibration characteristics of multi-body drill string system in oil and gas wells”, Nonlinear Dynamics 113, 19401–19434 (2025).